Basicity of Uranyl Oxo Ligands upon Coordination of Alkoxides

Marianne P. Wilkerson,[†,‡] Carol J. Burns,*[,†] Harry J. Dewey,[†] Jerod M. Martin,[†] David E. Morris,[†] Robert T. Paine,[‡] and Brian L. Scott[†]

Chemical Science and Technology Division, Los Alamos National Laboratory, Los Alamos, New Mexico 87545, and Department of Chemistry, University of New Mexico, Albuquerque, New Mexico 87131

Received February 9, 2000

Uranium(VI) alkoxide complexes are prepared via metathesis reactions of $[UO_2Cl_2(THF)_2]_2$ with potassium alkoxides in nonaqueous media. The dark red compound $U[OCH_2C(CH_3)_3]_6$, **1**, results from redistributive exchange of oxo and neopentoxide ligands between more than one uranium species. Single-crystal X-ray diffraction analysis of **1** reveals a monomer in which the uranium is coordinated in a pseudooctahedral fashion by six neopentoxide ligands. Imposition of steric congestion at the metal center prevents oxo−alkoxide ligand exchange in the reactions using more sterically demanding alkoxides. Simple metathesis between uranyl chloride and alkoxide ligands occurs in the synthesis of golden yellow-orange $UO_2(OCHPh_2)_2(THF)_2$, **2**, and yellow $UO_2[OCH(^tBu)Ph]_2(THF)_2$, **3**. Single-crystal X-ray diffraction analysis of **2** reveals a monomer in which the uranium is coordinated in a pseudooctahedral fashion by two apical oxo ligands, two diphenylmethoxide ligands occupying trans positions, and two tetrahydrofuran ligands. Coordination of diisopropylmethoxide allows for synthesis of a more complex binary alkoxide system. Single-crystal X-ray diffraction analysis of watermelon red $[UO_2(OCH(^iPr)_2)_2]_4$, **4**, reveals a tetramer in which each uranium is coordinated in a pseudooctahedral fashion by two apical oxo ligands, one terminal alkoxide, two bridging alkoxide ligands, and one bridging oxo ligand from a neighboring uranyl group. These compounds are characterized by elemental analysis, ^{1}H NMR, infrared spectroscopy, and, for **1**, **2**, and **4**, single-crystal X-ray diffraction analysis. Luminescence spectroscopy is employed to evaluate the extent of aggregation of compounds **2**−**4** in various solvents. Vibrational spectroscopic measurements of **2**−**4** imply that, in contrast to the case of uranyl complexes prepared in aqueous environments, coordination of relatively strongly donating alkoxide ligands allows for enhancement of electron density on the uranyl groups such that the uranyl U═O bonds are weakened. Crystal data are as follows. **1**: monoclinic space group $C2/m$, $a = 10.6192(8)$ Å, $b = 18.36(1)$ Å, $c = 10.6151(8)$ Å, $\beta = 109.637(1)°$, $V = 1949.1(3)$ Å^3, $Z = 2$, $d_{calc} = 1.297$ g cm^{-3}. Refinement of 2065 reflections gave R1 = 0.045. **2**: monoclinic space group $P2_1/c$, $a = 6.1796(4)$ Å, $b = 15.669(1)$ Å, $c = 16.169(1)$ Å, $\beta = 95.380(1)°$, $V = 1558.7(2)$ Å^3, $Z = 2$, $d_{calc} = 1.664$ g cm^{-3}. Refinement of 3048 reflections gave R1 = 0.036. **4**: tetragonal space group $I\bar{4}$, $a = 17.8570(6)$ Å, $b = 17.8570(6)$ Å, $c = 11.4489(6)$ Å, $V = 3650.7(3)$ Å^3, $Z = 2$, $d_{calc} = 1.821$ g cm^{-3}. Refinement of 1981 reflections gave R1 = 0.020.

Introduction

The chemistry of transition metal oxo species is often marked by the Lewis basic properties of the oxo ligand. It has been shown that a terminal oxo ligand can behave as an electron donor by bridging to either a homonuclear or heteronuclear Lewis acid,[1] while in the presence of a proton source, other metal oxo ligands may abstract a proton to form a hydroxide.[1f,2] The reactivity of this functional group has been exploited to effect a variety of stoichiometric and catalytic transformations, including nucleophilic attack on C−H bonds,[3] cycloaddition reactions,[1c,4] oxo metathesis or transfer,[4a,5] oxidation of hydrocarbons,[3b,c,6] and photolytic metal-to-oxo hydrocarbon migrations.[7] While the mechanisms are not completely understood, it is apparent that the transformations are influenced by the electronic nature of the coordinated ligands.

The most notable class of actinide oxo complexes to compare with their transition metal analogues is the actinyl ions, AnO_2^{n+}. In contrast to the transition metal oxo compounds, actinyl ions are considered to be thermodynamically and kinetically inert.[8] In addition, the strongly covalent bonding between the oxygen atoms and the uranium generally precludes another bonding interaction of the oxo ligands with a Lewis acid. Only limited examples, prepared either under elevated temperature/pressure or under nonaqueous reaction conditions, have been reported that exhibit coordination between a uranyl oxo ligand and another uranium.[9] More recently, terminal-oxo complexes of

* Corresponding author. E-mail: cjb@lanl.gov.
† Los Alamos National Laboratory.
‡ University of New Mexico.

(1) (a) Norquist, A. J.; Stern, C. L.; Poeppelmeier, K. R. *Inorg. Chem.* **1999**, *38*, 3448. (b) Hotzelmann, R.; Wieghardt, K.; Ensling, J.; Romstedt, H.; Gütlich, P.; Bill, E.; Flörke, U.; Haupt, H.-J. *J. Am. Chem. Soc.* **1992**, *114*, 9470. (c) Housmekerides, C. E.; Ramage, D. L.; Kretz, C. M.; Shontz, J. T.; Pilato, R. S.; Geoffroy, G. L.; Rheingold, A. L.; Haggerty, B. S. *Inorg. Chem.* **1992**, *31*, 4453. (d) Rau, M. S.; Kretz, C. M.; Mercando, L. A.; Geoffroy, G. L. *J. Am. Chem. Soc.* **1991**, *113*, 7420. (e) Pilato, R. S.; Rubin, D.; Geoffroy, G. L.; Rheingold, A. L. *Inorg. Chem.* **1990**, *29*, 1986. (f) Schreiber, P.; Wieghardt, K.; Nuber, B.; Weiss, J. *Polyhedron* **1989**, *8*, 1675. (g) West, B. O. *Polyhedron* **1989**, *8*, 219. (h) Yang, C.-H.; Ladd, J. A.; Goedken, V. L. *J. Coord. Chem.* **1988**, *19*, 235. (i) Rybak, W. K.; Ziółkowski, J. J. *J. Mol. Catal.* **1987**, *42*, 347. (j) Yang, C.-H.; Goedken, V. L. *Inorg. Chim. Acta* **1986**, *117*, L19. (k) Kress, J.; Wesolek, M.; Le Ny, J.-P.; Osborn, J. A. *J. Chem. Soc., Chem. Commun.* **1981**, 1039. (l) Schröder, M.; Nielson, A. J.; Griffith, W. P. *J. Chem. Soc., Dalton Trans.* **1979**, 1607. (m) Cartwright, B. A.; Griffith, W. P.; Schröder, M.; Skapski, A. C. *J. Chem. Soc., Chem. Commun.* **1978**, 853.

10.1021/ic000142u CCC: $19.00
Published on Web 10/27/2000

uranium have been generated which contain stronger σ-donor ligands.[10] Vibrational spectroscopy demonstrates a reduced metal−oxygen bond order in these species. It has also been determined that uranyl oxo ligands can display Brønsted basic character in alkaline environments.[11] These observations collectively suggest that appropriate coordination environments enhance the basicity of actinide oxo ligands. Further evidence for this phenomenon may be found in a structural report on $[UO_2(O^tBu)_2][UO(O^tBu)_4]_2$ (eq 1).[12]

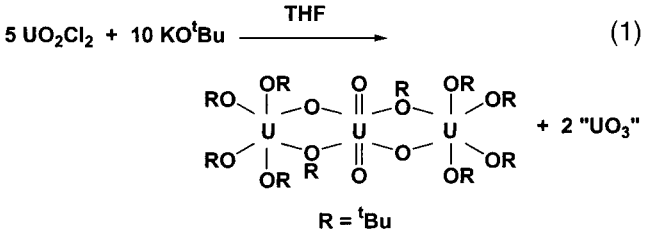

For instance, it has been reported that a binary uranyl alkoxide complex exchanges a bridging oxo ligand with alkoxide ligands of another uranyl complex, yielding a redistributed uranium oxo−alkoxide species and insoluble uranium oxide material.

To analyze the relative influence of electronic and steric effects supporting oxo-bridged species, we have prepared and characterized several new binary uranyl alkoxide and aryloxide complexes,[13] of which the alkoxide series will be discussed here. In one extreme, complete oxo−alkoxide ligand exchange to form hexakis(alkoxide) complexes is observed, while, in other cases, partial redistribution gives rise to polymetallic aggregates.[12] Control of redistributive exchange among uranyl alkoxide complexes may be exercised by the imposition of steric congestion at the alkoxide ligand. In the case of the diisopropylmethoxide ($OCH(^iPr)_2$) ligand, it is possible to isolate a base-free binary alkoxide, which exists in the solid state as a tetrameric aggregate with both bridging oxo and alkoxide ligands. In addition, vibrational spectroscopy is useful in determining the perturbation of U═O bonding induced by oxo bridging in the tetramer. Furthermore, it is possible to characterize aggregation of uranyl compounds in a variety of solvents through application of luminescence spectroscopy.[14]

Experimental Section

General Information. Standard inert-atmosphere techniques were used for the manipulation of all reactions.[15] ^{1}H NMR spectra (300 MHz) were recorded on a Varian UNITYplus-300 spectrometer. The chemical shifts are reported relative to the protio impurity of the deuterated solvent (C_6D_6, $\delta = 7.15$; THF-d_8, $\delta = 3.58$). All spectra were recorded at 298 K unless indicated otherwise. The samples were dissolved in a deuterated lock solvent and subsequently contained in sealed Teflon liners, which were then placed in 5 mm tubes. Infrared spectra were recorded on a Magna-IR system 750 spectrometer from Nujol mulls. Elemental analyses were performed in our laboratories on a Perkin-Elmer 2400 CHN analyzer. The samples were prepared and sealed in tin capsules in an inert-atmosphere box prior to combustion.

Continuous-wave (CW) luminescence data were obtained on a SPEX Industries Fluorolog 2 system consisting of a model 1680 two-stage 0.22 m emission monochromator. Samples were contained in sealed glass capillary tubes that were loaded under an inert atmosphere. All gratings were set to 1200 grooves/mm. The emitted light was detected by using a thermoelectrically cooled Hamamatsu model R928 photomultiplier tube with photon-counting electronics. The CW spectra were collected using the output from a 450 W Xe arc lamp. Luminescence data were obtained at approximately liquid-N_2 temperature using a simple insertion dewar and front-face collection optics. Integration times were 1−4 s/wavelength increment, and two to four spectra were typically averaged to derive each final spectrum. The emission data reported here have not been corrected for monochromator or detector response.

To extract vibrational data from the vibronically resolved emission spectra, the spectra were first transformed to the energy (cm^{-1}) domain.

(2) (a) Bélanger, S.; Beauchamp, A. L. *Inorg. Chem.* **1996**, *35*, 7836. (b) Mayer, J. M. *Polyhedron* **1995**, *14*, 3273. (c) Herrmann, W. A.; Fischer, R. A.; Amslinger, W.; Herdtweck, E. *J. Organomet. Chem.* **1989**, *362*, 333. (d) Cotton, F. A.; Wilkinson, G. *Advanced Inorganic Chemistry*; John Wiley & Sons: New York, 1988; Chapter 18. (e) Greenwood, N. N.; Earnshaw, A. *Chemistry of the Elements*; Pergamon Press: New York, 1984; Chapter 22.

(3) (a) Brown, S. N.; Myers, A. W.; Fulton, J. R.; Mayer, J. M. *Organometallics* **1998**, *17*, 3364. (b) Cook, G. K.; Mayer, J. M. *J. Am. Chem. Soc.* **1994**, *116*, 1855. (c) Lee, D. G.; Chen, T. *J. Am. Chem. Soc.* **1993**, *115*, 11231. (d) Haber, J.; Młodnicka, T. *J. Mol. Catal.* **1992**, *74*, 131.

(4) (a) Luo, L.; Lanza, G.; Fragalà, I. L.; Stern, C. L.; Marks, T. J. *J. Am. Chem. Soc.* **1998**, *120*, 3111. (b) Polse, J. L.; Andersen, R. A.; Bergman, R. G. *J. Am. Chem. Soc.* **1995**, *117*, 5393. (c) Bridgeman, A. J.; Davis, L.; Dixon, S. J.; Green, J. C.; Wright, I. N. *J. Chem. Soc., Dalton Trans.* **1995**, 1023. (d) Carney, M. J.; Walsh, P. J.; Hollander, F. J.; Bergman, R. G. *Organometallics* **1992**, *11*, 761. (e) Pilato, R. S.; Housmekerides, C. E.; Jernakoff, P.; Rubin, D.; Geoffroy, G. L.; Rheingold, A. L. *Organometallics* **1990**, *9*, 2333. (f) Pilato, R. S.; Geoffroy, G. L.; Rheingold, A. L. *J. Chem. Soc., Chem. Commun.* **1989**, 1287. (g) Jernakoff, P.; Geoffroy, G. L.; Rheingold, A. L.; Geib, S. J. *J. Chem. Soc., Chem. Commun.* **1987**, 1610.

(5) (a) Kwen, H.; Young, V. G., Jr.; Maatta, E. A. *Angew. Chem., Int. Ed. Engl.* **1999**, *38*, 1145. (b) Strong, J. B.; Haggerty, B. S.; Rheingold, A. L.; Maatta, E. A. *J. Chem. Soc., Chem. Commun.* **1997**, 1137. (c) Young, C. G.; Laughlin, L. J.; Colmanet, S.; Scrofani, S. D. B. *Inorg. Chem.* **1996**, *35*, 5368. (d) Laughlin, L. J.; Young, C. G. *Inorg. Chem.* **1996**, *35*, 1050. (e) Gable, K. P.; Juliette, J. J. J.; Li, C.; Nolan, S. P. *Organometallics* **1996**, *15*, 5250. (f) Stark, J. L.; Young, V. G., Jr.; Maatta, E. A. *Angew. Chem., Int. Ed. Engl.* **1995**, *34*, 2547. (g) Strong, J. B.; Ostrander, R.; Rheingold, A. L.; Maatta, E. A. *J. Am. Chem. Soc.* **1994**, *116*, 3601. (h) Holm, R. H.; Donahue, J. P. *Polyhedron* **1993**, *12*, 571. (i) Du, Y.; Rheingold, A. L.; Maatta, E. A. *J. Am. Chem. Soc.* **1992**, *114*, 345. (j) Legzdins, P.; Phillips, E. C.; Rettig, S. J.; Trotter, J.; Veltheer, J. E.; Yee, V. C. *Organometallics* **1992**, *11*, 3104. (k) Green, M. L. H.; Hogarth, G.; Konidaris, P. C.; Mountford, P. *J. Organomet. Chem.* **1990**, *394*, C9. (l) Holm, R. H. *Chem. Rev.* **1987**, *87*, 1401.

(6) (a) Goh, Y. M.; Nam, W. *Inorg. Chem.* **1999**, *38*, 914. (b) Cook, G. K.; Mayer, J. M. *J. Am. Chem. Soc.* **1995**, *117*, 7139.

(7) Brown, S. N.; Mayer, J. M. *Organometallics* **1995**, *14*, 2951.

(8) (a) Denning, R. G. *Struct. Bonding* (*Berlin*) **1992**, *79*, 215. (b) Denning, R. G. In *Gmelin Handbook of Inorganic Chemistry*; Buschbeck, K.-C.; Keller, C., Ed.; Springer-Verlag: Heidelberg, Germany, 1983; Vol. A6, p 31. (c) Gordon, G.; Taube, H. *J. Inorg. Nucl. Chem.* **1961**, *19*, 189.

(9) (a) Thuéry, P.; Nierlich, M.; Souley, B.; Asfari, Z.; Vicens, J. *J. Chem. Soc., Dalton Trans.* **1999**, 2589. (b) Rose, D.; Chang, Y.-D.; Chen, Q.; Zubieta, J. *Inorg. Chem.* **1994**, *33*, 5167. (c) Brandenburg, N. P.; Loopstra, B. O. *Acta Crystallogr.* **1978**, *B34*, 3734. (d) Ekstrom, A.; Loeh, H.; Randall, C. H.; Szego, L.; Taylor, J. C. *Inorg. Nucl. Chem. Lett.* **1978**, *14*, 301. (e) Taylor, J. C.; Ekstrom, A.; Randall, C. H. *Inorg. Chem.* **1978**, *17*, 3285. (f) Taylor, J. C.; Wilson, P. W. *Acta Crystallogr.* **1973**, *B29*, 1073. (g) Siegel, S.; Viste, A.; Hoekstra, H. R.; Tani, B. *Acta Crystallogr.* **1972**, *B28*, 117. (h) Siegel, S.; Hoekstra, H.; Sherry, E. *Acta Crystallogr.* **1966**, *20*, 292.

(10) (a) Arney, D. S. J.; Burns, C. J. *J. Am. Chem. Soc.* **1995**, *117*, 9448. (b) Arney, D. S. J.; Burns, C. J. *J. Am. Chem. Soc.* **1993**, *115*, 9840.

(11) Clark, D. L.; Conradson, S. D.; Donohoe, R. J.; Keogh, D. W.; Morris, D. E.; Palmer, P. D.; Rogers, R. D.; Tait, C. D. *Inorg. Chem.* **1999**, *38*, 1456.

(12) Burns, C. J.; Sattelberger, A. P. *Inorg. Chem.* **1988**, *27*, 3692.

(13) Wilkerson, M. P.; Burns, C. J.; Morris, D. E.; Paine, R. T.; Scott, B. L. Manuscript in preparation.

(14) (a) Moulin, C.; Laszak, I.; Moulin, V.; Tondre, C. *Appl. Spectrosc.* **1998**, *52*, 528. (b) Meinrath, G.; Kato, Y.; Kimura, T.; Yoshida, Z. *Radiochim. Acta* **1998**, *82*, 115. (c) Meinrath, G. *J. Radioanal. Nucl. Chem.* **1997**, *224*, 119. (d) Moulin, C.; Decambox, P.; Moulin, V.; Decaillon, J. G. *Anal. Chem.* **1995**, *67*, 348. (e) Morris, D. E.; Chisholm-Brause, C. J.; Barr, M. E.; Conradson, S. D.; Eller, P. G. *Geochim. Cosmochim. Acta* **1994**, *58*, 3613.

(15) Shriver, D. F.; Drezdzon, M. A. *The Manipulation of Air-Sensitive Compounds*, 2nd ed.; Wiley-Interscience: New York, 1986.

The data were fit to Gaussian model equations based upon empirical observations of the peaks. Gaussian fits were determined using a standard nonlinear least-squares curve-fitting routine available on IGOR[16] software running on a Macintosh platform.

The Raman spectroscopy was carried out using a microscope system or a macroscopic FT-Raman system. The microscope system consists of a Zeiss Axiovert 135TV inverted microscope equipped with a 20× objective (numerical aperture = 0.40). Raman scattered light was collected through a Kaiser Optical Systems Holospec holographic spectrometer equipped with a 752 nm holographic grating and imaged on a liquid-nitrogen-cooled Photometrics CH210 CCD with a 514 × 514 pixel chip. The spectrometer/CCD system was calibrated using the Raman spectrum of toluene. Samples were contained in sealed glass capillary tubes loaded under an inert atmosphere. All spectra were acquired with ∼15 mW power (measured at the sample) at 752 nm. Four to ten sets of spectra with 30−60 s integration times were collected and averaged. The FT-Raman system consists of a Nicolet model 960 FT-Raman spectrometer attached to a Nicolet model 560 Magna-IR instrument with an extended XT-KBr beam splitter and 180° sampling geometry. The excitation source is the 1064 nm light from a CW Nd:VO_4 laser. A 0.4 neutral density filter was used to decrease the laser power at the sample to ∼100 mW. The interferograms were detected with an InGaAs detector operated at room temperature. An average of 256 scans at 8 cm^{-1} resolution were taken to give each spectrum.

Materials. Anhydrous uranyl chloride bis(tetrahydrofuran) ($[UO_2Cl_2(THF)_2]_2$) was prepared by literature methods[17] from uranium oxide, purchased from Cerac. Potassium hydride, $HOCH_2C(CH_3)_3$, $HOCHPh_2$, HOCH(^{t}Bu)Ph, and HOCH(^{i}Pr)$_2$ were purchased from Aldrich. The alcohols were purified by either sublimation or distillation. The reagents $KOCH_2C(CH_3)_3$, $KOCHPh_2$, KOCH(^{t}Bu)Ph, and KOCH(^{i}Pr)$_2$ were prepared from the appropriate dry alcohol and KH in tetrahydrofuran at room temperature and were dried under vacuum. Solvents were rigorously dried by standard methods.[15]

Synthesis and Characterization. U[OCH$_2$C(CH$_3$)$_3$]$_6$ (1). $KOCH_2C(CH_3)_3$ (0.55 g, 4.4 mmol) was dissolved in THF (20 mL), and this solution was added to a solution of $[UO_2Cl_2(THF)_2]_2$ (1.00 g, 1.03 mmol) in THF (30 mL). The mixture was stirred for ∼1 h and then dried under vacuum. The solids were extracted with hexane (20 mL), and the extract was filtered through Celite. The dark red filtrate was concentrated to <10 mL and layered with a few drops of $HOCH_2C(CH_3)_3$, after which the mixture was cooled to −30 °C, yielding dark red blocks. A second crop was obtained by further reducing the volume of the solution to <5 mL and cooling. (Combined yield: 0.10 g, 0.13 mmol, 7%.) ^{1}H NMR (C_6D_6): δ = 7.52 (2H, s, $-CH_2-$), 1.12 (9H, s, $-CH_3$). IR (Nujol): 1730m, 1391m, 1349m, 1302sh, 1286w, 1261w, 1218w, 1168sh, 1149sh, 1137sh, 1116sh, 1052s, 1018s, 968w, 934w, 918w, 902w, 892sh, 876sh, 846w, 801m, 769w, 746m, 735sh cm^{-1}. Anal. Calcd for $C_{30}H_{66}O_6U$: C, 47.36; H, 8.74. Found: C, 47.28; H, 8.95.

UO$_2$(OCHPh$_2$)$_2$(THF)$_2$ (2). A solution of $KOCHPh_2$ (0.92 g, 4.1 mmol) dissolved in THF (20 mL) was added to a solution of $[UO_2Cl_2(THF)_2]_2$ (1.00 g, 1.03 mmol) in THF (30 mL). The mixture was stirred for ∼2 h and then filtered through Celite. The orange filtrate was concentrated to ∼5 mL and layered with a few drops of $HOCHPh_2$ and <1 mL of hexane, and the mixture was cooled to −30 °C, yielding golden yellow-orange bars (0.89 g, 1.1 mmol, 53%). ^{1}H NMR (C_6D_6): δ = 7.69−6.88 (11H, br m, $-C_6H_5$, −OCH overlapping), 3.58 (4H, br m, α-THF), 1.39 (4H, br m, β-THF). IR (Nujol): 1963w, 1942w, 1899w, 1888w, 1828w, 1675w, 1594m, 1581w, 1489s, 1341s, 1302m, 1282m, 1254m, 1222w, 1190w, 1181s, 1164m, 1156sh, 1148sh, 1117w, 1088s, 1054s, 1022s, 1001m, 989w, 976w, 968w, 937w, 922m, 915m, 908w, 878s, 871sh, 850m, 832m, 760s, 742s, 704s, 695s, 684s cm^{-1}. Anal. Calcd for $C_{34}H_{38}O_6U$: C, 52.31; H, 4.91. Found: C, 52.43; H, 5.18.

UO$_2$[OCH(^{t}Bu)Ph]$_2$(THF)$_2$ (3). A solution of KOCH(^{t}Bu)Ph (0.45 g, 2.2 mmol) dissolved in THF (20 mL) was added to a solution of $[UO_2Cl_2(THF)_2]_2$ (0.54 g, 0.55 mmol) in THF (20 mL). The mixture was stirred for ∼4 h and then filtered through Celite. The orange filtrate was concentrated to ∼5 mL and layered with a few drops of HOCH(^{t}Bu)Ph and <1 mL of hexane, after which the mixture was cooled to −30 °C, yielding yellow needles (0.20 g, 0.27 mmol, 25%). ^{1}H NMR (C_6D_6): δ = 7.82 (2H, br m, $-C_6H_5$), 7.10 (4H, m, $-C_6H_5$, −OCH overlapping), 3.60 (4H, br m, α-THF), 1.36 (9H, s, $-^t$Bu), 1.22 (4H, br m, β-THF). IR (Nujol): 2028w, 1958w, 1890w, 1598w, 1349s, 1309br, 1277w, 1198w, 1184w, 1170w, 1154w, 1144w, 1083s, 1052s, 1021sh, 1017s, 959w, 935w, 922w, 915w, 897w, 871s, 865sh, 834w, 788w, 767w, 743s, 706m, 666m cm^{-1}. Anal. Calcd for $C_{30}H_{46}O_6U$: C, 48.65; H, 6.26. Found: C, 48.18; H, 6.57.

[UO$_2$(OCH(^{i}Pr)$_2$)$_2$]$_4$ (4). KOCH(^{i}Pr)$_2$ (0.67 g, 4.3 mmol) was dissolved in THF (20 mL), and this solution was added to a solution of $[UO_2Cl_2(THF)_2]_2$ (1.03 g, 1.06 mmol) in tetrahydrofuran (40 mL). The mixture was stirred for 1 h and then filtered through Celite. The red filtrate was concentrated to ∼2 mL and layered with a drop of HOCH(O^{i}Pr)$_2$ and ∼5 mL of hexane, after which the mixture was cooled to −30 °C, yielding watermelon red blocks. A second crop was obtained by removing the solvents under vacuum, adding hexane (<5 mL), and recrystallizing at −30 °C. The combined yield was 0.33 g (0.16 mmol, 30%). ^{1}H NMR (C_6D_6): δ = 6.92 (1H, m, $^3J_{HH}$ = 6 Hz, −OCH), 6.52 (1H, m, $^3J_{HH}$ = 6 Hz, −OCH), 2.77 (1H, m, $^3J_{HH}$ = 6 Hz, −OCCH), 2.63 (1H, m, $^3J_{HH}$ = 6 Hz, −OCCH), 2.40 (2H, m, $^3J_{HH}$ = 6 Hz, −OCCH), 1.54 (6H, d, $^3J_{HH}$ = 6 Hz, $-CH_3$), 1.36−1.20 (9H, overlapping d, $^3J_{HH}$ = 6 Hz, $-CH_3$), 0.99−0.83 (9H, $^3J_{HH}$ = 6 Hz, overlapping d, $-CH_3$). ^{1}H NMR (THF-d_8): δ = 5.37 (1H, br m, −OCH), 2.06 (2H, br m, −OCCH), 1.22 (12H, d, $-CH_3$). IR (Nujol): 1958w, 1902w, 1647w, 1622w, 1353m, 1341m, 1317w, 1305w, 1294w, 1271w, 1263sh, 1181w, 1170w, 1158w, 1134m, 1101s, 1068w, 1013s, 991m, 985s, 958s, 946s, 923m, 907m, 861s, 837sh, 826w, 803w, 771w, 742s, 676s, 652m cm^{-1}. Anal. Calcd for $C_{56}H_{120}O_{16}U_4$: C, 33.61; H, 6.04. Found: C, 33.32; H, 6.21.

Crystallographic Measurements and Structure Solutions. Crystals of **1**, **2**, and **4** were obtained as described above. In each case, a single crystal was mounted on a glass fiber using silicone grease and placed under the −70 °C liquid N_2 vapor cold stream on a Siemens P4/CCD/PC diffractometer with a sealed Mo Kα X-ray source. A hemisphere of data was collected using a combination of ϕ and ω scans, with 30 s exposures and 0.3° frame widths. Data collection, indexing, and initial cell refinement were handled using SMART software,[18] frame integration and final cell refinement were carried out using SAINT software,[19] and the SADABS software package was used to perform the absorption corrections.[20] The structures were solved using Patterson and difference Fourier techniques.

The neopentoxide ligands of compound **1** were severely disordered. The neopentyl groups of the ligands were subsequently refined in two half-occupancy positions. Because of the disorder, the neopentyl carbon atoms were refined with isotropic temperature factors and hydrogen atoms were not considered in the model. The hydrogen atoms of compounds **2** and **4** were fixed in idealized positions, and the hydrogen atoms were refined using a riding model, with isotropic temperature factors fixed to 1.2 times the isotropic U_{eq} values of the carbon atoms to which they were bonded. The final refinements of compounds **2** and **4** included anisotropic temperature factors for all non-hydrogen atoms. Refinements were carried out using SHELXTL 5.1 software.[21] Refinement by full-matrix least-squares techniques based on F^2 converged with R1 = 0.045 and wR2 = 0.118 (**1**), R1 = 0.036 and wR2 = 0.106 (**2**), and R1 = 0.020 and wR2 = 0.042 (**4**). Additional data collection and structure refinement details are given in Table 1, and pertinent bond distances and angles are summarized in Tables 2 and 3.

(16) *IGOR Pro 3.12*; WaveMetrics, Inc.: Lake Oswego, OR.
(17) Wilkerson, M. P.; Burns, C. J.; Paine, R. T.; Scott, B. L. *Inorg. Chem.* **1999**, *38*, 4156.
(18) *SMART*, Version 4.210; Bruker Analytical X-ray Systems: Madison, WI, 1996.
(19) *SAINT*, Version 4.05; Bruker Analytical X-ray Systems: Madison, WI, 1996.
(20) Sheldrick, G. *SADABS*; University of Göttingen: Göttingen, Germany, 1996.
(21) *SHELXTL*, Version 5.1; Bruker Analytical X-ray Systems: Madison, WI, 1997.

Table 1. Crystal and Structure Refinement Data for $U[OCH_2C(CH_3)_3]_6$ (**1**), $UO_2(OCHPh_2)_2(THF)_2$ (**2**), and $[UO_2(OCH(^iPr)_2)_2]_4$ (**4**)

	1	**2**	**4**
empirical formula	$C_{30}H_{66}O_6U$	$C_{34}H_{38}O_6U$	$C_{56}H_{120}O_{16}U_4$
fw	760.8	780.7	2001.6
temp, °C	−70	−70	−70
wavelength, Å	0.710 73	0.710 73	0.710 73
crystal system	monoclinic	monoclinic	tetragonal
space group	*C*2/*m*	$P2_1/c$	$I\bar{4}$
a, Å	10.6192(8)	6.1796(4)	17.8570(6)
b, Å	18.36(1)	15.669(1)	17.8570(6)
c, Å	10.6151(8)	16.169(1)	11.4489(6)
β, deg	109.637(1)	95.380(1)	
volume, Å^3	1949.1(3)	1558.7(2)	3650.7(3)
Z	2	2	2
d_{calc}, g cm^{-3}	1.297	1.664	1.821
abs coeff, mm^{-1}	4.191	5.249	8.899
F(000)	640	764	1904
crystal size, mm	0.19 × 0.17 × 0.20	0.17 × 0.07 × 0.09	0.10 × 0.07 × 0.08
θ range, deg	2.04−26.39	1.81−26.39	1.61−26.42
limiting indices	$-13 \le h \le 12$	$-7 \le h \le 7$	$-15 \le h \le 15$
	$0 \le k \le 22$	$0 \le k \le 9$	$0 \le k \le 22$
	$0 \le l \le 13$	$0 \le l \le 20$	$0 \le l \le 14$
no. of reflns collected	2065	3048	1981
no. of data/restraints/params	2065/0/82	3048/0/187	1981/0/173
goodness-of-fit on F^2	0.985	0.881	0.940
final R^a indices [$I > 2\sigma(I)$]: R1, wR2	0.045, 0.118	0.036, 0.106	0.020, 0.042
x	0.1	0.1	0.0303
R^a indices (all data): R1, wR2	0.045, 0.119	0.064, 0.125	0.023, 0.044
largest diff peak and hole, e Å^{-3}	1.323 and −0.620	0.677 and −0.791	0.387 and −0584

[a] $R1 = \sum||F_o| - |F_c||/\sum|F_o|$; $wR2 = [\sum w(F_o^2 - F_c^2)^2/\sum w(F_o^2)^2]^{1/2}$, and $w = 1/[\sigma^2(F_o^2) + (xP)^2]$.

Table 2. Selected Bond Lengths (Å) and Angles (deg) for $U[OCH_2C(CH_3)_3]_6$ (**1**)

U−O(1)	2.002(10)	U−O(2)	2.001(8)
O(1)−U−O(1A)	180.0	O(2)−U−O(2A)	180.0
O(1)−U−O(2)	90.6(7)	O(2)−U−O(2B)	91.0(11)
O(1)−U−O(2A)	89.4(7)	O(2)−U−O(2C)	89.0(11)
O(1)−U−O(2B)	89.4(7)	U−O(1)−C(1)	147(3)
O(1)−U−O(2C)	90.6(7)	U−O(2)−C(6)	145(2)

Results and Discussion

The recently reported complex $[UO_2Cl_2(THF)_2]_2$ has proven to be a valuable reagent for probing the alkoxide chemistry of the uranyl ion in nonaqueous media.[17] The complex is readily soluble in THF and reacts with a variety of alkoxide salts to generate products of metathesis. As has been previously noted,[12] reactions of uranyl chloride with less bulky alkoxide ligands can give rise to products arising from oxo−alkoxide ligand redistributive exchanges. In the present study, the reaction of $[UO_2Cl_2(THF)_2]_2$ with potassium neopentoxide also gives, as the sole isolable species, a uranyl complex generated by replacement of each oxo ligand by two alkoxide groups: uranium(VI) hexakis(neopentoxide), **1** (eq 2). The high solubility

$$^3/_2[UO_2Cl_2(THF)_2]_2 + 6KOCH_2C(CH_3)_3 \xrightarrow{THF} \underset{\mathbf{1}}{U[OCH_2C(CH_3)_3]_6} + 6KCl + 2\text{“}UO_3\text{”} \quad (2)$$

of **1** and the byproducts from the reaction account for the low total yield of **1** (7% based on $^1/_2$ $[UO_2Cl_2(THF)_2]_2$). (The maximum theoretical yield of **1**, based on the stoichiometry in eq 1, is 33%.) The byproducts of this reaction are potassium chloride and an insoluble orange precipitate that is found to be amorphous by powder X-ray diffraction. Elemental analysis confirms that the precipitate is not strictly UO_3. The carbon and hydrogen contents (as high as 14.81 % C, and 2.80 % H) demonstrate the presence of some residual hydrocarbon, presumably owing to inclusion of limited amounts of neopentoxide-containing products. There is no evidence of reduction of the uranium on the basis of optical and vibrational spectroscopy.

The ^{1}H NMR spectrum of **1** displays one set of resonances for all neopentoxide ligands. There are no resonances in the spectrum that can be attributed to free or coordinated tetrahydrofuran. Indeed, there have been earlier examples of uranium(VI) hexakis(alkoxides) reported in the literature, although these examples were isolated in higher yields via oxidation of $U(OCH_3)_6^{2-}$ or metathesis of UF_6.[22] As has been observed for other homoleptic U(VI) alkoxide complexes, the infrared spectrum of **1** is relatively simple, the most notable feature being the ν(O−C) bands at 1052 and 1018 cm^{-1},[23] the former of which is identical to the ν(O−C) stretching frequency, 1051.5 cm^{-1}, observed for the methoxide analogue, $U(OMe)_6$.[22c] The additional band at 1018 cm^{-1} observed for **1** but not for $U(OMe)_6$ could be due to relaxation of the point group of **1** or to $U(OMe)_6$ having a low-intensity fundamental vibration not observed.[24] As expected, there is no evidence of uranyl U═O stretching modes.

The molecular structure of **1** is shown in Figure 1. The uranium is coordinated in a pseudooctahedral fashion by six alkoxide oxygen atoms. The U−O distances are 2.001(8) and 2.002(10) Å. These values are slightly shorter than the average

(22) (a) Coroiu, I.; Demco, D. E.; Bogdan, M.; Darabont, A. *Rom. J. Phys.* **1997**, *42*, 665. (b) Bursten, B. E.; Casarin, M.; Ellis, D. E.; Fragalà, I.; Marks, T. J. *Inorg. Chem.* **1986**, *25*, 1257. (c) Cuellar, E. A.; Miller, S. S.; Marks, T. J.; Weitz, E. *J. Am. Chem. Soc.* **1983**, *105*, 4580. (d) Marks, T. J.; Cuellar, E. A.; Miller, S. S.; Weitz, E. U.S. Patent 4,-364,870, 1982. (e) Jacob, E. *Angew. Chem., Int. Ed. Engl.* **1982**, *21*, 142. (f) Cuellar, E. A.; Marks, T. J. *Inorg. Chem.* **1981**, *20*, 2129. (g) Miller, S. S.; DeFord, D. D.; Marks, T. J.; Weitz, E. *J. Am. Chem. Soc.* **1979**, *101*, 1036. (h) Jones, R. G.; Bindschadler, E.; Blume, D.; Karmas, G.; Martin, G. A., Jr.; Thirtle, J. R.; Yeoman, F. A.; Gilman, H. *J. Am. Chem. Soc.* **1956**, *78*, 6030.

(23) Nakamoto, K. *Infrared and Raman Spectra of Inorganic and Coordination Compounds*, 4th ed.; John Wiley & Sons: New York, 1986.

(24) Lowering the symmetry of an idealized O_h complex to D_{4h} produces a splitting of the normal mode T_{1u} to $A_{2u} + E_u$: Cotton, F. A. *Chemical Applications of Group Theory*; John Wiley & Sons: New York, 1990; Appendix IIB.

Table 3. Selected Bond Lengths (Å) and Angles (deg) for $UO_2(OCHPh_2)_2(THF)_2$ (**2**) and $[UO_2(OCH(^iPr)_2)_2]_4$ (**4**)

		2		**4**
U═O	U═O(1)	1.779(5)	U(1)═O(1)	1.846(4)
			U(1)═O(2)	1.783(4)
U−O	U−O(2)	2.168(4)	U(1)−O(3)	2.065(5)
	U−O(3)	2.416(5)	U(1)−O(4)	2.289(4)
			U(1)−O(1A)	2.435(4)
			U(1)−O(4A)	2.427(4)
O═U═O	O(1)═U═O(1A)	180.0	O(1)═U(1)═O(2)	172.6(2)
U−O−C	U(1)−O(2)−C(1)	130.3(4)	U(1)−O(3)−C(3)	175.8(5)
			U(1)−O(4)−C(8)	125.1(4)
			U(1B)−O(4)−C(8)	133.2(4)
O−U−O	O(3)−U−O(3A)	180.0	O(1)−U(1)−O(3)	93.1(2)
	O(1)−U−O(2)	88.8(2)	O(1)−U(1)−O(4)	76.0(2)
	O(1)−U−O(3)	89.9(2)	O(1)−U(1)−O(1A)	86.4(2)
	O(2)−U−O(3)	88.0(2)	O(1)−U(1)−O(4A)	87.8(2)
			O(2)−U(1)−O(3)	92.3(2)
			O(2)−U(1)−O(4)	97.9(2)
			O(2)−U(1)−O(1A)	89.0(2)
			O(2)−U(1)−O(4A)	95.5(2)
			O(3)−U(1)−O(4)	103.7(2)
			O(3)−U(1)−O(1A)	170.5(2)
			O(3)−U(1)−O(4A)	106.7(2)
			O(4)−U(1)−O(1A)	85.39(14)
			O(4)−U(1)−O(4A)	146.1(2)
			O(1A)−U(1)−O(4A)	63.81(14)
U−O−U			U(1)−O(1)−U(1B)	116.7(2)
			U(1)−O(4)−U(1B)	101.7(2)

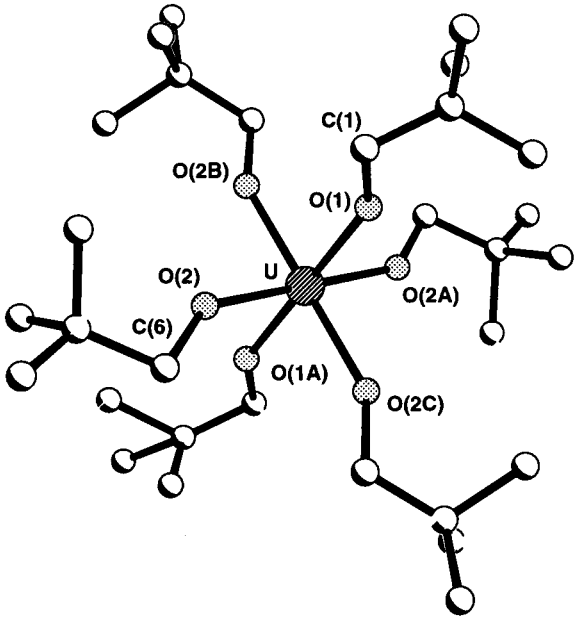

Figure 1. Atom-labeling scheme for $U[OCH_2C(CH_3)_3]_6$.

U−O bond length in $U(OCH_3)_6$ (2.10 Å).[22b] The U−O−C bond angles of **1** are slightly more bent at 147(3) and 145(2)° when compared with the average U−O−C bond angle of 153.7° for $U(OCH_3)_6$.

Compound **1** results from ligand exchange between uranyl oxo ligands and neopentoxide ligands. While there are other rare examples of products resulting from redistributive exchanges of uranyl oxo ligands and alkoxides reported in the literature,[12,25] the majority of the solid state structures of uranyl compounds exhibit arrangements in which there is no direct bonding interaction between uranyl moieties. Two classes of alkoxides have been identified that effectively prevent redistribution. The first contains less basic ligands, such as aryloxides or fluoroalkoxides.[13,26] Presumably, the somewhat more electronegative substituents on these ligands (relative to aliphatic ligands) do not increase the electron density on the metal as much, resulting in tighter bonding between the uranium and oxo ligands.

Another means of preventing oxo−alkoxide ligand exchange is imposition of steric congestion at the metal center.[27] This result has been demonstrated in the isolation of monomeric uranium alkoxides containing strongly coordinating bases (eq 3).[28] It is also conceivable that redistribution would be inhibited

$$UO_2Cl_2(OPPh_3)_2 + 2KO^tBu \xrightarrow{THF} UO_2(O^tBu)_2(OPPh_3)_2 + 2KCl \quad (3)$$

by inclusion of sterically encumbered alkoxide ligands. To test this possibility, metathesis reactions of the uranyl ion with a series of bulky alkoxide ligands were examined. The reaction of $[UO_2Cl_2(THF)_2]_2$ with potassium diphenylmethoxide permits isolation of the simple metathesis product $UO_2(OCHPh_2)_2(THF)_2$, **2** (eq 4). The product may exist as either the *cis*- or

$$^1/_2[UO_2Cl_2(THF)_2]_2 + 2KOCHPh_2 \xrightarrow{THF} \underset{\mathbf{2}}{UO_2(OCHPh_2)_2(THF)_2} + 2KCl \quad (4)$$

trans-bis(alkoxide) complex; the ^{1}H NMR data do not allow an unambiguous assignment of the geometry of the alkoxide product in solution. Therefore, a single-crystal X-ray diffraction analysis of **2** was undertaken.

As expected, compound **2** exists as a uranyl monomer (Figure 2). The uranium atom is coordinated in a pseudooctahedral fashion, with oxo ligands in trans-axial positions. Because the uranium atom lies on a crystallographic center of symmetry, the O−U−O angle is rigorously linear. The uranyl U−O(1) bond length is 1.779(5) Å. This distance is similar to the values reported for six-coordinate $UO_2(O^tBu)_2(OPPh_3)_2$ (1.789(5) and

(25) Bradley, D. C.; Chatterjee, A. K.; Chatterjee, A. K. *J. Inorg. Nucl. Chem.* **1959**, *12*, 71.

(26) Andersen, R. A. *Inorg. Chem.* **1979**, *18*, 209.

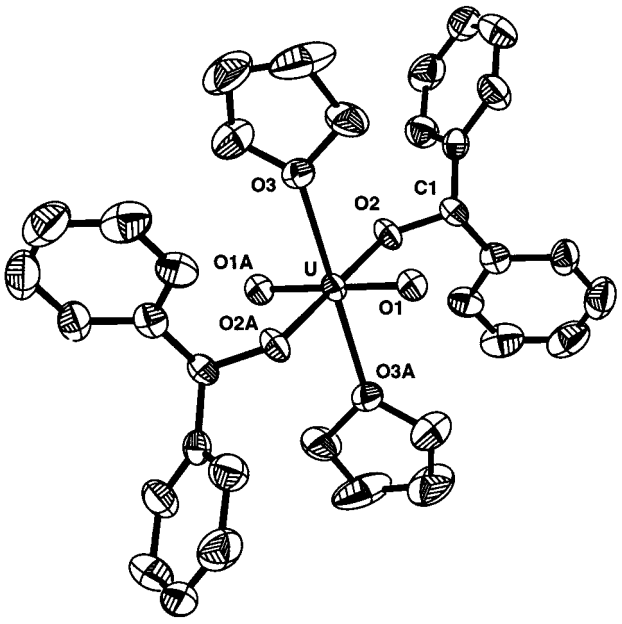

Figure 2. Thermal ellipsoid drawing of $UO_2(OCHPh_2)_2(THF)_2$ showing the atom-labeling scheme used in the tables (50% probability ellipsoids).

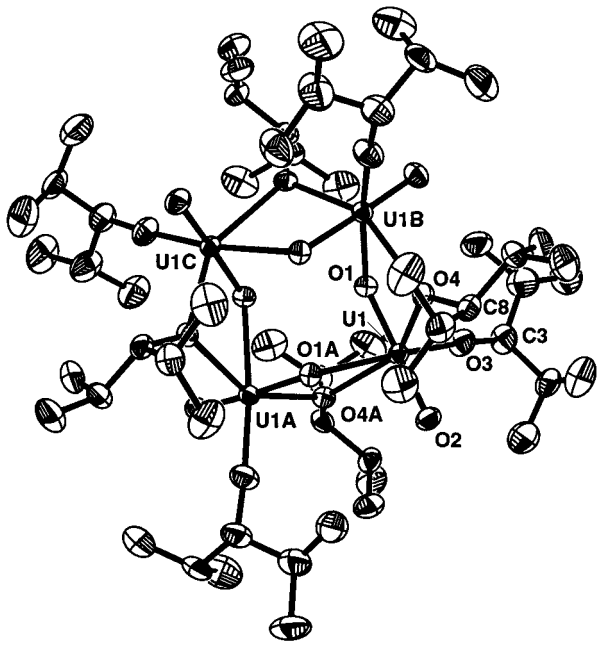

Figure 3. Thermal ellipsoid drawing of $[UO_2(OCH(^iPr)_2)_2]_4$ showing the atom-labeling scheme used in the tables (50% probability ellipsoids).

1.795(6) Å).[28] The two alkoxide ligands are arranged trans to one another. The U−O(alkoxide) bond distance, 2.168(4) Å, is similar to the U−O(terminal alkoxide) lengths for $UO_2(O^tBu_2)_2(OPPh_3)_2$ (2.143(6) and 2.162(6) Å). These bond distances are slightly longer than the U−O(terminal alkoxide) bond lengths of $[UO_2(O^tBu_2)_2][UO(O^tBu)_4]_2$, which span the range 2.015(6)−2.055(6) Å.[12] This apparent lengthening may be due to interligand crowding generated by the larger alkoxide ligands. The angle about the alkoxide oxygen atoms (e.g., U−O(2)−C(1) = 130.3(4)°) are smaller than those found for $UO_2(O^tBu_2)_2(OPPh_3)_2$ (148.3(6) and 140.6(6)°) and $[UO_2(O^tBu_2)_2][UO(O^tBu)_4]_2$ (151.6(7)−163.1(8)°). The U−O(tetrahydrofuran) bond distances in **2** (2.416(5) Å) are within the range of values reported for other uranyl−tetrahydrofuran distances reported in the literature (2.32(3)−2.49(4) Å).[29]

It must be noted that the diphenylmethoxide ligand is likely to be less donating than saturated alkoxide ligands,[30] and there may be an electronic argument for the lack of observed ligand exchange (as has been observed in uranyl fluoroalkoxide chemistry).[26] It is observed, however, that replacement of one phenyl substituent by a *tert*-butyl group does not promote redistributive exchange either. The reaction of $[UO_2Cl_2(THF)_2]_2$ with potassium *tert*-butylphenylmethoxide in THF similarly results in the formation of the monomer $UO_2[OCH(^tBu)Ph]_2(THF)_2$, **3** (eq 5). An attempt was made to determine the

$$^1/_2[UO_2Cl_2(THF)_2]_2 + 2KOCH(^tBu)Ph \xrightarrow{THF} \underset{\mathbf{3}}{UO_2[OCH(^tBu)Ph]_2(THF)_2} + 2KCl \quad (5)$$

structure of **3** by single-crystal X-ray diffraction. The X-ray data collected for **3** were of poor quality and allowed only the atom connectivities within the molecule to be determined. There was additional electron density that could not be accounted for, which precluded satisfactory convergence of the model. The data did unambiguously confirm the trans arrangement of *tert*-butylphenylmethoxide ligands in the equatorial plane of the molecule, identical to the molecular structure obtained for the compound $UO_2(OCHPh_2)_2(THF)_2$, **2**.

When saturated alkoxide ligands of even greater steric bulk are employed,[31] the extent of redistributive exchange and aggregation appears to be a more complex function of ligand solubility, as well as steric size. In most systems, discrete products of partial redistribution are recrystallized,[12] while, in other systems, products simply consisting of binary uranyl alkoxides are isolated. In both cases, there is evidence of some ligand exchange, indicated by the presence of insoluble amorphous byproducts as described above. However, unlike compounds **2** and **3**, these species are not monomeric; the size and/or basicity of the ligand promote the formation of aggregates containing bridging oxo and alkoxide ligands. An example of this may be seen in the reaction of $[UO_2Cl_2(THF)_2]_2$ with potassium diisopropylmethoxide (eq 6). The only product

$$^1/_2[UO_2Cl_2(THF)_2]_2 + 2KOCH(^iPr)_2 \xrightarrow{THF} \underset{\mathbf{4}}{[UO_2(OCH(^iPr)_2)_2]_4} + 2KCl \quad (6)$$

crystallized from this reaction is the binary complex $[UO_2(OCH(^iPr)_2)_2]_4$, **4**.

Compound **4** exists as a tetrameric aggregate in the solid state (Figure 3). The tetramer consists of four uranyl groups related by an S_4 axis; the uranium atoms (U(1), U(1A), U(1B), U(1C)) are arranged in a nearly planar, square configuration (maximum deviation from the plane = 0.192 Å). The coordination geometry

(27) Leciejewicz, J.; Alcock, N. W.; Kemp, T. J. *Struct. Bonding* (*Berlin*) **1995**, *82*, 43.

(28) Burns, C. J.; Smith, D. C.; Sattelberger, A. P.; Gray, H. B. *Inorg. Chem.* **1992**, *31*, 3724.

(29) Charpin, P.; Lance, M.; Nierlich, M.; Vigner, D.; Baudin, C. *Acta Crystallogr.* **1987**, *C43*, 1832.

(30) pK_a values of the related alcohols: $HOCH_2CH_2CH_3$, 16.1; $HOCH_2Ph$, 15.4. See: Serjeant, E. P.; Dempsey, B. *Ionisation Constants of Organic Acids in Aqueous Solution*; Pergamon Press: New York, 1979.

(31) Within the alkoxide series, the relative sizes of the ligands were determined by measuring the largest "cone angle" occupied by the alkoxide ligands (including the van der Waals radii of the hydrogen atoms) coordinated to uranyl groups, yielding the order $OCH_2CMe_3 < OC(Me_3)_3 < OCH(^iPr)_2$.

around each uranium atom can be regarded as a distorted octahedron with trans uranyl oxo ligands in the apical positions. The uranyl groups are now quite asymmetric, however. The terminal U(1)−O(2) bond length is 1.783(4) Å, which is within the estimated standard deviation of the bond length determined for the U═O bond length of **2**, while the bridging U(1)−O(1) bond distance is 1.846(4) Å, which compares well with other U═O(bridging) distances.[9] The oxo bridge is also quite asymmetric. The U←O bond distance is significantly longer at 2.435(4) Å. There is no direct U−U contact (U(1)···U(1A) = 3.6570(3) Å). In the limited number of solid-state structures in which uranyl oxo ligands serve as equatorial ligands to neighboring uranium atoms, the dative O→U distances range from 2.30(2) to 2.54(3) Å.[9] These lengths are similar to the distance found between a uranium(VI) atom and a coordinating THF molecule. The uranyl O═U═O angle remains nearly linear (172.6(2)°).

The equatorial plane of each uranyl group is completed by one terminal alkoxide and two bridging alkoxide ligands. The terminal alkoxide oxygen−uranium distance is 2.065(5) Å, which is somewhat shorter than the U−O(alkoxide) bond length of **2**. The bridging alkoxide U(1)−O(4) bond length of 2.289(4) Å is longer than the terminal U−O alkoxide distances, as would be expected. The angle about each terminal alkoxide oxygen atom (e.g., U−O(3)−C(3) = 175.8(5)°) is nearly linear. It is much larger than the U−O−C alkoxide bond angle for **2**, likely as a consequence of steric interactions between the alkyl group with the bridging diisopropylmethoxide ligands. Close nonbonded contacts observed in the structure include C(1B)−C(9A) (3.855 Å), C(1B)−C(10C) (3.698 Å), C(3B)−C(9A) (3.687 Å), and C(5B)−C(7) (3.880 Å); these are all significantly shorter than the distance expected for the sum of the van der Waals radii of two methyl groups (4.0 Å).[32]

It is significant to note that, although the product is isolated in the presence of excess tetrahydrofuran, the uranyl oxo ligands are apparently sufficiently basic that they compete favorably with the THF for coordination to the Lewis acidic metal centers. As discussed above, the uranyl oxo ligand is only rarely reported to act as a Lewis base toward a neighboring metal center, and in most cases, these compounds are prepared under high temperature/pressure or in nonaqueous solution.[9] Furthermore, the bonding mode of tetrameric **4** provides evidence for proposed redistribution intermediates of uranyl alkoxide aggregates.[12] For example, it has been suggested that the reaction pathways for the synthesis of redistribution products involve formation and dimerization of $UO_2(OR)_2(THF)_x$ through bridging oxo ligands, followed by decomposition to $UO(OR)_4$ and insoluble UO_3. In the case where R = ^{t}Bu, the intermediate $UO(OR)_4$ reacts with $UO_2(OR)_2$ to form $[UO_2(O^tBu)_2][UO(O^tBu)_4]_2$. When R = $CH_2C(CH_3)_3$, $UO(OR)_4$ dimerizes with $UO_2(OR)_2$ through bridging oxo ligands and the complex then redistributes to $U[OCH_2C(CH_3)_3]_6$ and an additional equivalent of UO_3 (Figure 4).

The basicity of these oxo ligands presumably results either from charge repulsion between the oxo ligands and the more basic uranium or from competition between the oxo ligands and the equatorial alkoxides for π-symmetry U 6d and 5f orbitals, resulting in a weakening of the uranyl U−O bond. A sensitive indicator of this bond strength lies in the Raman stretch of O═U═O. The symmetric stretch for compound **4** is observed at 713 cm^{-1}, a dramatic change from the average ν_1 for the uranyl group (~860 cm^{-1})[23] and a value lower than ν_1 reported for

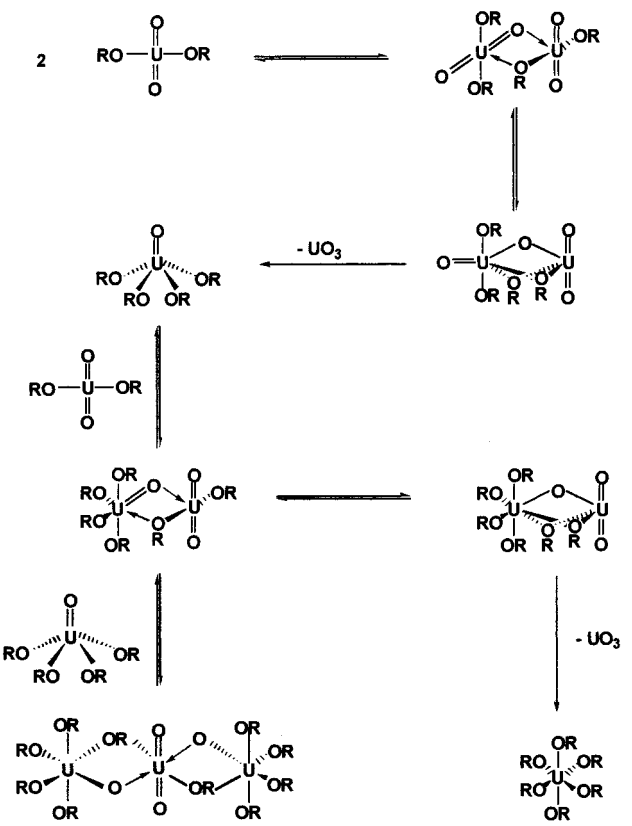

Figure 4. Proposed mechanisms for the redistribution of uranyl bis(alkoxides).

any uranyl complex. Presumably, the large reduction of the uranyl symmetric stretch of **4** is more greatly influenced by coordination to a neighboring Lewis acid than by coordination of strongly donating ligands. While the symmetric stretches of the monomeric compounds **2** and **3** (804 and 796 cm^{-1}, respectively) also lie at lower energy than the average ν_1, they are not shifted to the red as effectively as ν_1 for compound **4**.

Interestingly, different ^{1}H NMR spectra were observed in noncoordinating versus coordinating solvents. The spectrum of **4** obtained in benzene-d_6 at room temperature was complex but showed the presence of two alkoxide environments, consistent with coordination of a terminal and a bridging alkoxide in a 1:1 ratio. Variable-temperature ^{1}H NMR spectra (cyclohexane-d_{14} from −100 to +70 °C) did not reveal any chemical exchange between terminal and bridging alkoxide ligands and exhibited only sharpening of resonances as the high-temperature limit was approached. However, further analysis of the room-temperature ^{1}H NMR spectrum of **4** in tetrahydrofuran-d_8 yielded a different signature, revealing only one diisopropylmethoxide environment. Therefore, an investigation into the properties of this molecular aggregate in both noncoordinating and coordinating solvents was undertaken.

A particularly informative tool for characterization of the environment of uranyl ions both in the solid state and in solution is optical spectroscopy. A distinguishing feature of the optical spectra of uranyl compounds is the presence of a weak low-energy peak (520 → 370 nm) ascribable to a symmetry-forbidden HOMO−LUMO electronic transition from a σ_u-HOMO to a δ_u-LUMO.[8a] It is often observed (at least at low temperature) that this absorption may be resolved into a series of vibronic bands, with an energy spacing corresponding to ν_1(O═U═O) of the electronically excited uranyl ion. In addition, this excited state is often relatively long-lived ($t_{1/2} \geq 100$ ms),[33] permitting the observation of emission back to the ground state.[34]

(32) Pauling, L. *The Nature of the Chemical Bond*, 3rd ed.; Cornell University Press: Ithaca, NY, 1960.

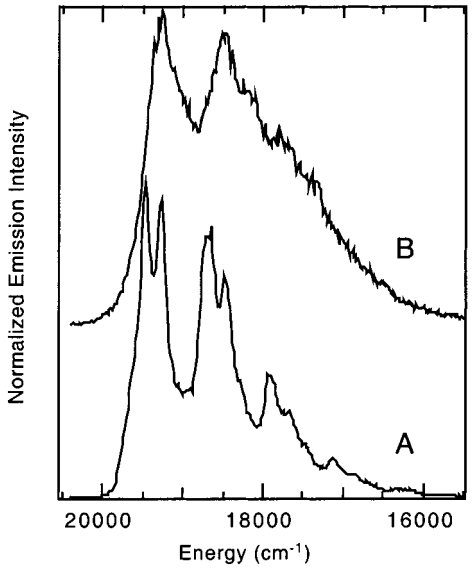

Figure 5. Electronic emission spectra of $UO_2(OCHPh_2)_2(THF)_2$ (**2**) for a neat sample (A) and for a 0.0040 M tetrahydrofuran solution (B). Both spectra were obtained at liquid-nitrogen temperature.

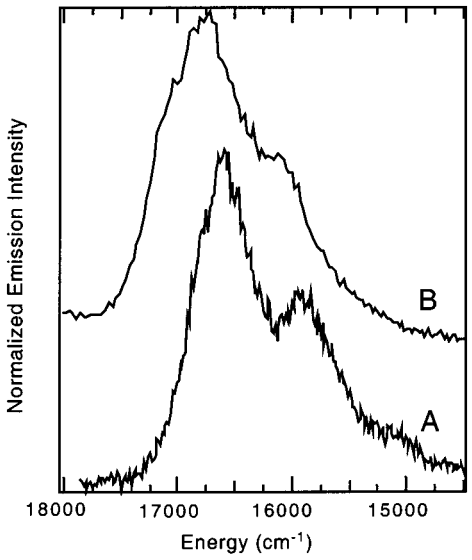

Figure 6. Electronic emission spectra of $[UO_2(OCH(^iPr)_2)_2]_4$ (**4**) for a neat sample (A) and for a 0.0040 M benzene solution (B). Both spectra were obtained at liquid-nitrogen temperature.

Emission spectroscopy has been employed to provide key information regarding the electronic environment of the uranyl ion in solution, including the extent of aggregation. Frequently, one or more vibronic bands are superimposed on the electronic emission envelope, the most prominent being due to the totally symmetric ν_1 mode of the O═U═O moiety. Meinrath reported that hydrolytic uranyl species exhibit a red shift in the absorption maximum with an increase in oligomerization.[14c] Morris,[14e] and Moulin[14a,d] also observed this feature in the emission spectra of more hydrolyzed and presumably more oligomeric species. While the hydrolysis chemistry of the uranyl ion is not structurally analogous to the chemistry of these nonaqueous systems, we attempted to determine if the spectroscopic trends observed in our nonaqueous systems are comparable.

As a benchmark for the spectroscopic manifestations of oligomerization, the monomeric species, **2** and **3**, were examined first. The luminescence spectra for **2** at liquid-nitrogen temperature are shown in Figure 5. For clarity, these spectra were normalized with respect to the emission intensity. Spectrum A shows the emission of the neat monomeric solid at 77 K. This spectrum has a well-resolved vibronic structure with the calculated E_{0-0} at ~19 470 cm^{-1} and vibronic progressions in two modes: one at ~780 cm^{-1}, which we attribute to the ν_1 mode, and a second at ~200 cm^{-1}, which we assign to the bending ν_2 mode.[34] Spectrum B was obtained for a solution of **2** in tetrahydrofuran (0.004 M). This spectrum has an apparent E_{0-0} at 19 290 cm^{-1} and a single resolved progression with a vibronic spacing of ~780 cm^{-1}. The modest 180 cm^{-1} shift in E_{0-0} for spectrum B relative to spectrum A is probably a consequence of solvation effects. The intensity of the solution spectrum is also substantially diminished, suggesting enhanced nonradiative decay processes in solution. However, the similarity of the spectral envelopes and the vibronic spacing of ~780 cm^{-1} for spectra A and B are consistent with a single, dominant uranyl species, the monomer **2**. The vibronic spacing of ~780 cm^{-1} is comparable to the Raman measurement of ν_1 for both the neat solid and the tetrahydrofuran solution (804 cm^{-1}). In comparison, the emission spectra of **3** (not shown) have an apparent E_{0-0} at ~19 190 cm^{-1} in the solid state and an E_{0-0} at ~19 140 cm^{-1} in tetrahydrofuran (0.004 M). The apparent vibronic spacing of 800 cm^{-1} in both the neat solid state and tetrahydrofuran solution is in excellent agreement with the Raman measurement of ν_1 (796 cm^{-1}).

The liquid-nitrogen-temperature luminescence spectra of the neat solid and the benzene solution of **4** (0.0040 M) are shown in Figure 6, A and B, respectively. Spectrum A has an E_{0-0} at ~16 610 cm^{-1} and a single resolved progression with a vibronic spacing of ~710 cm^{-1}, in excellent agreement with ν_1 (713 cm^{-1}) determined by Raman spectroscopy. Spectrum B has an E_{0-0} at 16 870 cm^{-1} and a vibronic progression of ~710 cm^{-1}. As mentioned above, the 260 cm^{-1} shift in E_{0-0} for spectrum B relative to spectrum A is most likely attributable to solvation effects. However, the approximate E_{0-0} of **4** (~16 610 cm^{-1}) relative to that of monomer **2** (~19 480 cm^{-1}) represents a dramatic red shift of ~2870 cm^{-1}. The direction of the shift is the same as that observed with an increasing degree of aggregation in aqueous uranyl solutions, and indeed, the shift is even greater.

Because of the variation in ^1H NMR spectra of **4** in noncoordinating versus coordinating solvents, the luminescence of **4** in tetrahydrofuran was examined. Should tetrahydrofuran solvation of **4** induce deaggregation of the tetramer, the new species would be predicted to emit at energies between ~19 470 and 16 610 cm^{-1}. The 77 K luminescence spectra from a dilution series of **4** are shown in Figure 7. It is readily apparent that there are at least two species in solution, one for which the spectrum has a vibronic structure with an apparent E_{0-0} at ~17 160 cm^{-1} and a vibronic spacing of ~780 cm^{-1} and a second whose spectrum occurs at a higher energy with an apparent E_{0-0} at ~19 010 cm^{-1} and a vibronic spacing of ~850 cm^{-1}. In addition, the higher energy spectrum is blue-shifted by 2400 cm^{-1} relative to that of the tetrameric molecule. Since the energy of the latter emission spectral component is close to that of monomeric compound **2** (E_{0-0} = 19 470 cm^{-1}), it is postulated that this spectral component is attributable to a

(33) Baird, C. P.; Kemp, T. J. *Prog. React. Kinet.* **1997**, *22*, 87.

(34) The exact location of the electronic origin (E_{0-0}) is frequently difficult to discern in UO_2^{2+} spectra, at the level of resolution obtained here. In particular, for systems with rigorous inversion symmetry (e.g., **2**), the 0−0 transition is forbidden and the initial (high-energy) intensity frequently arises in a vibronic transition[8a] one quantum lower in energy than E_{0-0}. Here we report apparent E_{0-0} values based on the location of the first vibronic band. The exact position of the electronic origin could lie at higher energy.

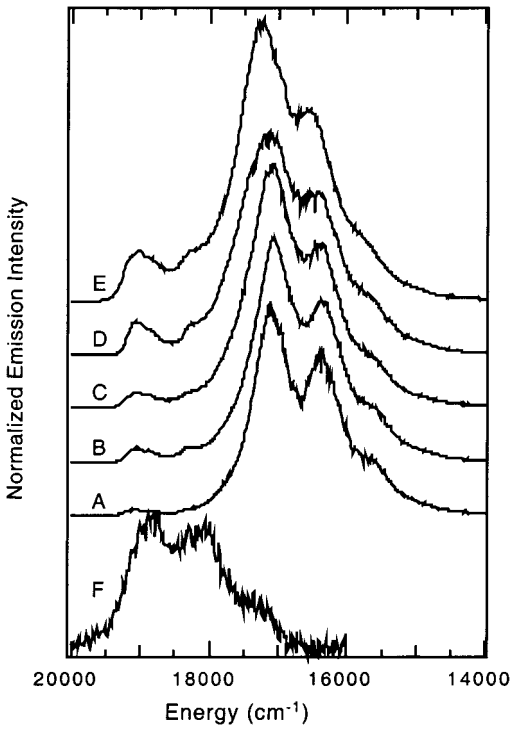

Figure 7. Electronic emission spectra of $[UO_2(OCH(^iPr)_2)_2]_4$ (**4**) for tetrahydrofuran solutions: A, 0.0200 M; B, 0.0120 M; C, 0.0080 M; D, 0.0040 M; E, 0.0010 M; F, 0.0004 M. Spectra were obtained at liquid-nitrogen temperature. Spectra A−E were manipulated so that the low-energy spectral edges coincided to facilitate comparison of the two principal components. The intensity of spectrum F was multiplied by 500 to illustrate relative peak positions.

monomer. While the spectral component with E_{0-0} at 17 160 cm^{-1} is only 550 cm^{-1} higher in energy than that of the tetrameric species, the difference in vibronic spacing (780 vs 710 cm^{-1}) rules out the possibility that this spectrum arises from the tetramer. It is probable that the species responsible for this lower energy spectrum is intermediate in nuclearity (i.e., dimeric or trimeric), although it is not possible to clarify the nature of the bridging interation (oxo versus alkoxide) from these data. In a dilution series of luminescence spectra, it is obvious that as the concentration of **4** is decreased from 0.0200 to 0.0004 M, there is an increase in the presence of this predicted monomer relative to the amount of the second species. Therefore, the dissolution of **4** in coordinating tetrahydrofuran induces deaggregation by solvation, and the resulting equilibrium is strongly dependent on the total concentration. In the extreme, i.e., upon crystallization, the complex reverts to the tetrameric form.

Conclusions

It has been shown that coordination of more basic ligands allows for the enhancement of electron density on the uranyl ion such that the oxo ligands exhibit properties consistent with increased basicity. This effect increases the propensity of the uranyl oxo ligands to bridge between metal centers and, in the extreme, results in ligand redistribution between uranium intermediates. Such oxo exchange allows for the formation of unusual coordination environments not obtained for uranyl compounds in aqueous media. In the presence of a primary alkoxide, complete oxo−alkoxide exchange to yield the U(VI) hexakis(alkoxide) compound is facile. Control over redistributive behavior may be influenced by the introduction of steric bulk and ligand solubility. The coordination of a very bulky alkoxide prevents redistribution completely, yielding complexes of the formula $UO_2(OR)_2L_2$ (L = solvent). Use of a highly soluble and sterically large saturated alkoxide creates the serendipitous situation where redistribution is inhibited but the metal center remains sufficiently coordinatively unsaturated to permit aggregation by means of bridging oxo and alkoxide ligands. This results in the isolation of the novel tetrameric compound **4**.

Raman and emission spectroscopies have elucidated several features of the tetramer, **4**. The uranyl U═O bond strength of **4** is weakened presumably owing to a combination of ligand basicity and intermolecular oxo bridging. The level of aggregation of these uranyl alkoxides may be elucidated by comparison of the relative shifts of the E_{0-0} transitions. The emission profiles of **4** in the solid state and in a noncoordinating solvent glass are comparable, while the emission of **4** in tetrahydrofuran is considerably blue-shifted owing to deaggregation of the molecule. It is readily apparent that there exists an equilibrium involving an as yet unidentified uranyl diisopropylmethoxide species in tetrahydrofuran solution as a function of uranyl concentration. It may be possible to observe the effects of the enhanced Lewis basicity of the oxo ligands in the reactivity of this molecule. We have seen indications that the chemical properties of these uranyl species may be comparable to the reactivities of transition metal oxo species. We are currently pursuing investigations of the chemical behavior of these species.

Acknowledgment. This research at Los Alamos National Laboratory was supported by the Division of Chemical Energy Sciences, Office of Basic Energy Sciences, U.S. Department of Energy, and by the Laboratory Directed Research and Development Program. Los Alamos National Laboratory is operated by the University of California for the U.S. Department of Energy under Contract W-7405-ENG-36.

Supporting Information Available: X-ray crystallographic files, in CIF format, for **1**, **2**, and **4**. This material is available free of charge via the Internet at http://pubs.acs.org.

IC000142U